Arabian Journal of Chemistry (2023) **16**, 104551

King Saud University

Arabian Journal of Chemistry

www.ksu.edu.sa
www.sciencedirect.com

ORIGINAL ARTICLE

Enhanced skin anti-inflammatory and moisturizing action of gold nanoparticles produced utilizing *Diospyros kaki* fruit extracts

Sanjeevram Dhandapani [a], Rongbo Wang [a], Ki cheol Hwang [b], Hoon Kim [c,*], Yeon-Ju Kim [a,*]

[a] *Graduate School of Biotechnology, and College of Life Science, Kyung Hee University, Yongin-si, 17104, Gyeonggi-do, Republic of Korea*
[b] *Rafarophe Co, Venture Research Center, Cheongju, Republic of Korea*
[c] *Department of Food and Nutrition, Chung Ang University, Seodong-daero 4726, Daedeok-myeon, Anseong 17546, Republic of Korea*

Received 4 October 2022; accepted 4 January 2023
Available online 10 January 2023

KEYWORDS

Persimmon fruit extract;
Biosynthesized AuNPs;
HaCaT keratinocytes;
Skin disorders;
MAPK/NF-κB;
PI3K/Akt

Abstract Inflammatory skin diseases (ISD) cause very severe itchy skin and dryness which is now a days an important issue which has to be taken care. Nanotechnology plays a main role in manufacturing cosmetic ingredients at a nanoscale size. Among different nanoparticles, gold (Au) is one of the non-toxic materials synthesized organically or inorganically. For synthesizing nanoparticles (NPs), using inorganic methods may cause some toxicity to cells, but using organic synthesis like plant extract is less toxic and environmentally friendly. Therefore, we synthesized DK-AuNPs using *Diospyros kaki* fruit extract. UPLC-MS/MS was used to evaluate phytochemicals responsible for converting salt into nanoparticles. The DK-AuNPs were characterized to confirm the formation of NPs. Furthermore, we analyzed the activity of DK-AuNPs on human keratinocytes (HaCaT cells). The DK-AuNPs showed 98.2 % cell survival upto 200 μg/mL against HaCaT cells. Additionally, compared to DK treatment, DK-AuNPs therapy decreased ROS production in TNF-α/IFN-γ (T + I) stimulated HaCaT cells by 68.7 %, whereas DK treatment reduced ROS generation by 27.8 %. Moreover, the skin anti-inflammatory potential and moisturizing effect of DK-AuNPs were analyzed using HaCaT cells. Furthermore, skin inflammatory activity biomarkers were downregulated through the MAPK/NFκB signaling pathway and showed significant inhibition by DK-AuNPs. Also, the skin moisturizing biomarkers such as HAS (1–3) were upregulated and HYAL

* Corresponding authors at: Graduate School of Biotechnology, and College of Life Science, Kyung Hee University, Yongin-si, 17104, Gyeonggi-do, Republic of Korea.
E-mail addresses: saphead1106@hanmail.net (H. Kim), yeonjukim@khu.ac.kr (Y.-J. Kim).
Peer review under responsibility of King Saud University.

Production and hosting by Elsevier

https://doi.org/10.1016/j.arabjc.2023.104551

(1–2) were downregulated by PI3K/AKT/NFκB through HAS2 regulation. Therefore, skin anti-inflammatory and moisturizing activity were enhanced by treatment with DK-AuNPs. In summary, we conclude that the DK-AuNPs could be a new alternative for skin disease.

1. Introduction

Inflammatory skin disease (ISD) is a chronic, recurring, and acute inflammatory itchy skin condition that is caused by the breakdown of the skin barrier which is a complex and composite condition (Torres et al., 2019). Under pathological conditions *trans*-epidermal water loss (TEWL) occurs resulting in dryness, and inflammation increases, resulting in the release of inflammatory mediators (Klonowska et al., 2018). Inflammatory mediators including cytokines and chemokines which are produced by inflammatory macrophages such as keratinocytes, mast cells, langerhans cells, lymphocytes and neutrophils, resulting in an anti-dermatitis effect (Asahina & Maeda, 2017). Keratinocytes are essential for skin homeostasis because of its role in the recruitment of immune cells, including neutrophils, monocytes, and T lymphocytes, via the production of chemokines and cytokines (Maalej et al., 2022). Therefore, suppression of pro-inflammatory cytokines and chemokines could be essential in the treatment of ISD.

For decades, nanoparticles (NPs), ranging from 1 to 100 nm in size, have been widely used in numerous sectors (Cho et al., 2022; Contini et al., 2020). Because of their excellent targeting ability, nano-drug delivery systems can be highly beneficial in pharmaceutical and biotechnological applications (Mirzaei et al., 2016). Several studies have shown that nanoparticles and nanocarriers have optimum rheological qualities, antibacterial capabilities, and the potential to repair skin conditions (Damiani et al., 2019). Several reports have been published regarding the use of nanoparticles, nanogels, nanomixtures, nanoemulsions, and other nanocarrier dermatitis treatments (Ferreira et al., 2021). According to the current study, nanoparticles such as silver nanoparticles (Ag-NPs), silver-lipid, and poly (lactic acid) nanoparticles (PLA-NPs) have been proven for the treatment and management of people suffering from dermatitis (Rujido-Santos et al., 2019).

In recent years, the use of gold nanoparticles (AuNPs) in biological applications (Akhtar et al., 2022; Gessner et al., 2022; Iranpour Anaraki et al., 2022), such as drug delivery, antibacterial, and anticancer agent, has become popular (Ahati et al., 2022; Nagaraj et al., 2022; Qu et al., 2022; Sekar et al., 2022). AuNPs have a therapeutic drug delivery mechanism that includes anti-inflammatory and immune response modulation. These mechanisms indicate prospective applications for AuNPs as "drugs" to treat a variety of skin disorders (Ko et al., 2022). Wang et al. reported AuNPs synthesized using *Rosa rugosa* extract could able to supprelss skin inflammation in HaCaT Keratinocytes (Wang et al., 2022). Similary, Xu et al. showed that ani-dermatitis effect was enhanced by treating AuNPs mediated by plant extract (Xu et al., 2022). Therefore, AuNPs have become a major topic in the field of nanosystem development and use for topical drug administration becasuse their biocompatibility, tunability in size and surface chemistry, and distinctive plasmonic characteristic (Chen & Feng, 2022). However, inadequate research has been performed on the anti-dermatitis effects of nano drugs containing gold nanoparticles for inflammatory skin conditions and skin moisturizing effects. Synthesis of AuNPs typically occurs via various traditional physical and chemical processes, many of which involve the use of hazardous substances that possesses risks to human health and contribute to the environmental pollution (Mishra et al., 2020). Compared to nanomaterials produced by chemical synthesis, nanoparticles produced through biosynthesis have gained considerably more attention (Botteon et al., 2021; Song et al., 2022; Zayadi & Bakar, 2020). Biosynthesis methods involve the use of naturally available metabolites from plants and microorganisms such as bacteria, fungi, and algae for synthesizing AuNPs in an environmentally friendly manner (Sanjeevram et al., 2021 Xu et al., 2021). The plant extract was used to synthesize NPs (Doan et al., 2021), which have been demonstrated to be more promising than those that are synthesized using inorganic procedures in terms of biocompatibility and bioactivity (Marcelino et al., 2021). Plant extracts contain various macromolecules from complex characteristic categories, including alkaloids, polysaccharides, vitamins, amino acids, proteins, enzymes, tannins, phenolic acids, saponins, and naturally occurring substances (Vandarkuzhali et al., 2021). Additionally, the plant extract's secondary metabolites concurrently stabilised and capping the zero-valent species of Au^0, resulting in the production of AuNPs (M. Wang et al., 2021). Based on the findings of several studies, researchers have proved that the vast majority of the above molecules are environmentally friendly, which are responsible for biosynthesis of nanoparticles (Pradeep et al., 2021).

Diospyros kaki (DK; persimmon) is a well-known and widely cultivated plant species. Its fruit is recognized as one of the most important fruits in terms of both quantity and economic importance. In recent years, interest in investigating the chemical and bioactive content of DK fruit has grown worldwide. Several studies have been conducted on the impact of DK fruits and their compounds on human health. The main components of DK fruit are carbohydrates, organic acids, phenolic compounds, carotenoids, and tannins, which impart antioxidant, anticancer, and pharmacological properties to the fruit. Moreover, it has several macro and micronutrients with excellent bioavailability (Matheus et al., 2020). It was reported that both the fruit and the leaves of the DK have significant biological importance, including anti-inflammatory properties, protection against atherosclerosis, reduction in cholesterol levels, resistance to free radicals, protection against diabetes, treatment of cancer, and prevention of cancer. Lydia Ferrara gave a clear and brief description of the DK significance, both in terms of the nutritional advantages and the potential pharmaceutical uses (Ferrara, 2021). Direito et al. demonstrated that the administration of DK extract attenuates the degree of chronic inflammation and tissue damage typical of CIA in rats (Direito et al., 2020). The current attention in dermatological and cosmeceutical disciplines has been directed towards the utilization of natural bioactive substances in several therapeutic and beautifying applications. Scientific evidence has shown DK exhibited benifits in the fields of dermatology and cosmetics, which makes it a desirable alternative. The DK fruit contains a variety of essential micronutrients, including potassium, sodium, iron, and calcium. The fruit has been a main component in various commercially available cosmetic goods, such as soaps, body lotions that cleanse and fragrance, body washes, skin tones, and body serums (Kashif et al., 2017).

Therefore, In this research, we aimed to biosynthesize AuNPs containing DK fruit extract (DK-AuNPs) and evaluating their effects on dermatitis symptoms, such as inflammation and dehydration. In addition, the mechanism underlying its anti-inflammatory effects and hyaluronic acid (HA) synthesis in HaCaT cells has been examined. Therefore, according to the findings of our research, this is the first study to demonstrate the properties of AuNPs mediating DK fruit extract that are capable of reducing inflammation and hydrating the skin.

2. Materials and methods

2.1. Extraction of DK and synthesis of DK-AuNPs

2.1.1. DK extract phytochemical identification and DK-AuNPs synthesis

The fresh DK fruits were gathered from the farm of Sanju aram dried persimmon farming association (Gyeongbuk, South Korea) in the year 2020. After that, the fruits were allowed to air-dry at room temperature for up to sixty days. Then 3 kg of dry DK were washed with water to eliminate any surface impurities, and refluxing at 107 °C for 4 h in a commercial biofeedback extractor manufactured by Daehan Media Co., ltd. (Gunpo, South Korea). Finally, DK was lyophilization using a freeze-dryer (Ilshin Biobase Co., ltd., Dongducheon, South Korea) and a brief description was given in our previous study (Hwang et al., 2021; Shin et al., 2022). Analytical methods and conditions for identifying secondary metabolites in DK using ultra-performance liquid chromatography-tandem mass spectrometry (UPLC-MS/MS; LTQ Orbitrap XL) manufactured by Thermo Electron (Waltham, MA, USA), according to standard analytical methods and conditions (Hwang et al., 2021; Kim et al., 2021). DK-AuNPs were biosynthesized and optimized under various conditions, including different gold salt concentrations; DK fruit extract concentrations; and reaction parameters such as pH, temperature, and time. DK concentrations of 6 mg/mL–9 mg/mL and $HAuCl_4{\cdot}3\ H_2O$ concentrations of 1–5 mM. We performed the synthesis under temperatures ranging from 50 to 80 °C and reaction times varying from 5 to 20 min. The synthesized DK-AuNPs were collected, washed thrice with autoclaved water, and centrifuged for 15 min at 13,000 rpm. For subsequent experiments, the DK-AuNPs were stored at 4 °C. The reduction of the metal ions was measured using ultraviolet–visible spectroscopy (Optizen POP; Mecasys, Daejeon, Korea) at wavelengths between 300 and 800 nm.

2.1.2. Physicochemical characterization of DK-AuNPs

An X-ray diffractometer (XRD, D8 Advance (Bruker), Karlsruhe, Germany) with an operating temperature range of 20–80 °C was used for obtaining an XRD pattern of the synthesized DK-AuNPs sample. The organic compounds encapsulated on the exterior of the DK-AuNPs were classified using Fourier-transform infrared (FT-IR, Spectrum One System (Perkin-Elmer), Waltham, MA, USA) spectroscopy in the range of 4,000–500 cm^{-1} and at a resolution of 4 cm^{-1}. Structural and compositional analyses, selected area electron diffraction (SAED), and energy-dispersive X-ray (EDX) spectroscopy of the gold nanoparticles were performed using transmission electron microscopy (TEM, JEM-2100F, Tecnai G2 Spirit, FEI Company, USA) with negative staining of the gold nanoparticles. Droplets of pure nanoparticles dispersed in water were placed on a carbon-coated copper grid and dried at room temperature before TEM imaging. The size and dispersal nature of the nanoparticles were determined using a dynamic light scattering (DLS, ELS-2000ZS, Otsuka Electronics, Shiga, Japan) particle analyzer.

2.2. Assessment of DK-AuNPs cytotoxicity

2.2.1. Cytotoxic effect of DK-AuNPs in HaCaT cells

HaCaT cells (human keratinocytes) were provided by CLS Cell Line Service (Eppelheim, Heidelberg, Germany). The cells were seeded in Dulbecco's Modified Eagle Medium (DMEM) with 10 % heat-inactivated FBS and 1 % PS and maintained at 37 °C in a humidified incubator under 5 % CO_2. A standard MTT test was performed for determining the cytotoxicity. In a 96-well plate, cells were seeded at an initial density of 1×10^5 cells/well and stabilized. The cells were treated with varying concentrations (10 – 800 μg/mL) of DK fruit extract and DK-AuNPs. After 24 h of treatment, the cells were treated with 3-(4,5-Dimethylthiazol-2-yl)-2,5-Diphenyltetrazolium Bromide (MTT) solution (5 mg/mL) for 1 h, and the resultant formazan crystals were dissolved in 100 μL of Dimethyl sulfoxide (DMSO). A microplate reader (SpectraMax® ABS Plus, San Jose, CA, USA) was used for measuring the absorbance at 570 nm.

2.2.2. Live and dead staining

Cell viability was assessed using a live/dead cell imaging kit (Invitrogen Biotechnology, Waltham, MA, USA). Live cells were labeled green, while dead cells were stained red. The cells were loaded into the microfluidic devices, and after one day, we washed the culture flasks of the microfluidic chip with phosphate-buffered saline (PBS, HyClone) for 1–3 min. The cells were then incubated for 15–30 min at 37 °C with the reagent from the live/dead cell imaging kit. After washing off the reagent with PBS for 3–5 min, we examined the culture chambers under a fluorescence microscope. Finally, the proportion of green fluorescence in all cells was used for determining cell viability.

2.3. Evaluation of skin anti-inflammatory activity and skin moisturizing effects

2.3.1. Reactive oxygen species (ROS) and Mito-SOX quantification

Intracellular ROS release was identified using a Cellular ROS/Superoxide Detection Assay Kit, which was provided by Abcam (Cambridge, MA, USA). HaCaT cells (1×10^5 cells) were cultured in 6-well plates and treated for 24 h with varying concentrations of DK, DK-AuNPs, TNF-α/IFN-γ (T + I) and dexamethasone (DEX - Positive control (PC)). Then, 0.4 μL of oxidative stress and superoxide detection reagents were added to the mixture. After an incubation period of 30 min, the fluorescence was measured using a microscope (Leica Microsystems, Wetzlar, Germany).

2.3.2. Enzyme-linked immunosorbent (ELISA) analysis

Cells were seeded in a 96-well plate at a density of 1×10^5 cells/well. After 24 h, the cells were pretreated with DK-AuNPs and DK at different doses (100 and 200 μg/mL, respectively) for 1 h before being treated with T + I. Following the manufacturer's instructions, the supernatants were collected and tested for the production of pro-inflammatory cytokines or chemokines and hyaluronan acid production (HA), using an ELISA

assay kit (R&D Systems, Minneapolis, MN, USA). Table S2 lists the quantitative ELISA kits used in this study.

2.3.3. Quantitative real-time PCR

HaCaT cells were plated onto plates and cultured for 24 h. The cells were treated with the sample and cultured for an additional 24 h after the culture medium was changed. Total mRNA was isolated from the cells. TRIzol lysis solution was added after two rounds of PBS washes (Invitrogen, Carlsbad, CA, USA). A first-strand synthesis kit was used for reverse-transcribing RNA into cDNA (Invitrogen, USA). SYBR® Green Sensimix plus Master Mix was used for quantitative real-time PCR (qRT-PCR, Quantace, Watford, UK). The primer sequences are listed in Supplementary Table S3 and were provided by Macrogen (Seoul, Republic of Korea). The threshold cycle (Ct) was estimated for each reaction using the $2 - \Delta\Delta Ct$ method ($\Delta\Delta Ct = \Delta Ct[\text{treated}] - \Delta Ct[\text{control}]$). The gene encoding β-actin served as the housekeeping gene in this experiment.

2.3.4. Western blotting

For this experiment, HaCaT cells were cultured for 24 h, following which they were treated with the samples for another 24 h after the culture medium was changed. Radioimmunoprecipitation assay (RIPA) lysis buffer (ThermoFisher Scientific, Waltham, MA, USA) was used for extracting total protein from the cells after two rounds of PBS rinsing. We used a protein gel electrophoresis chamber system (Thermo Fisher Scientific) to separate equal quantities (50 µg) of total protein on a sodium dodecyl sulfate (SDS) polyacrylamide gel containing 10 % SDS, before transferring the separated proteins to a polyvinylidene fluoride membrane. PBS with 5 % skimmed milk was used for blocking the blots for 1 h at room temperature before primary antibodies were added and incubated overnight at 4 °C. Incubation with HRP-conjugated secondary antibody was followed by washing with Tris-buffered saline containing 0.1 % Tween 20 on the membrane, was completed after 1 h. Table S4 lists the antibodies used for this study. Thermo Fisher Scientific's Enhanced Chemiluminescence reagent was used for detecting the protein bands, and Image J was used for quantifying bands.

2.4. Statistical analysis

Three independent experiments were performed in triplicate, and the results are presented as mean standard deviation (SD). We used GraphPad Prism 8 to perform statistical calculations and Student's *t*-test to determine significant differences. The significance level was set at $p < 0.05$ for all differences.

3. Results and discussion

3.1. Synthesis of DK-AuNPs

The biosynthesis of DK-AuNPs was evaluated under various conditions (Schwartz-Duval et al., 2020), and the obtained results are shown in Fig. 1. The multiple conditions were examined which includes acidity, synthesis time, metal salt (Au) concentration, and DK concentration during biosynthesis of DK-AuNPs. The final optimal conditions listed in Table S1 were selected for the synthesis of DK-AuNPs. According to the TEM images, the DK-AuNPs were polygonal, triangular, hexagonal, sperical or elliptical in morphology, with mean size 23.42 ± 12.6 nm (Fig. 2A). According to the EDX spectra, the transmittance peaks for gold and copper were the highest, peaking at 2.1b and 8 keV, respectively (Fig. 2B). The copper

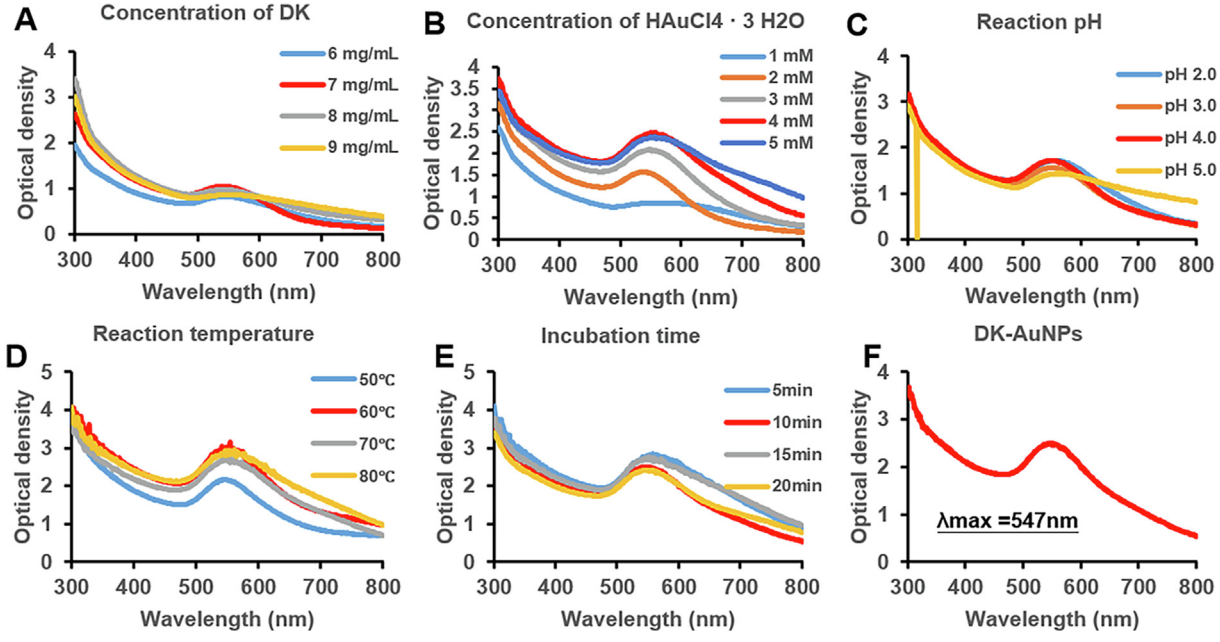

Fig. 1 Based on the dynamic level of absorption, as absorbs using UV–vis spectroscopy, the synthesis procedure for DK-AuNPs was optimized. (A) DK was used at concentrations ranging from 6 to 9 mg/mL (B) The influence of varying concentrations of gold salt (1–5 mM). (C) The implications of pH fluctuations (pH 2–5). (D) The consequence of temperature fluctuations (50–80 °C). (E) The impact of the incubation period (5–20 min). (F) The UV absorbance of the optimized DK-AuNPs.

grid employed for TEM structural research has been shown to generate a copper peak (Dhandapani et al., 2021). The crystallographic structure of the DK-AuNPs was determined using XRD and SAED. The four primary peaks of the gold nanoparticles at 38.14°, 44.31°, 64.55°, and 77.59° corresponded to the 111, 200, 220, and 311 planes of Bragg's reflection (Fig. 2C and 2D). The FT-IR spectrum of the samples was assessed using an open spectral library for bioactive compounds and the FT-IR spectrum database for identifying their chemical bonds. The samples exhibited distinct patterns (Fig. 3A). The peaks at 3326.38 cm^{-1} and 3325.57 cm^{-1} in DK and DK-AuNPs are attributed to phenolic and aliphatic hydroxyl groups, respectively. The C — H stretch of the methylene groups of the protein was related to the bands at 2932.56 cm^{-1} in DK and 2930.23 cm^{-1} in DK-AuNPs (R. Wang et al., 2021). The stretched C═O group is identifiable by the band that may be found for DK at 1716.52 cm^{-1}. The existence of the C═C bond of benzene is possibly responsible for the peak at 1615.48 cm − 1 in DK-AuNPs and that at 1591.36 cm^{-1} in DK. The CH bending vibration results from the presence of alkenes and aliphatic amine functional groups, and it can be identified by the signals at 1403.99 cm^{-1}, 1314.88 cm^{-1}, and 1038.46 cm^{-1} in DK and those at 1445.50 cm^{-1}, 1376.80 cm^{-1}, 1229.05 cm^{-1}, and 1073.9 cm^{-1} in DK-AuNPs. DLS spectroscopy showed that the DK-AuNPs were 219.5 nm in intensity and 85.5 nm in volume (Fig. 3B). TEM and DLS were used to measure the molecular size; however, the findings might vary. DLS analysis shows size distribution depending on the conjugated diameter or hydrodynamic size in colloidal particles; hence, the sizes are quite often greater than those according to TEM analysis.

3.2. Evaluating the cytotoxic effect of DK-AuNPs

The MTT assay was used to compare the cytotoxicity in HaCaT cells treated with DK-AuNPs and DK. The cells were treated with varying concentrations of DK-AuNPs and DK (10–800 μg/mL) for 24 h. DK-AuNPs showed a lower inhibitory effect at high concentrations, and DK produced no cytotoxic effect (Fig. 4A). Thus, compared to DK alone, DK-AuNPs showed no harmful impact at low concentrations. Finally, for future experiments, we used non-toxic concentrations of DK-AuNPs and DK (100 and 200 μg/mL, respectively). Additionally, we used LIVE/DEAD staining for confirming the cytotoxic effect of DK-AuNPs and DK (Fig. 4B). The red color indicated dead cells, while the green cells were alive. DK-AuNPs and DK did not significantly affect cell death. Collectively, our findings indicated that converting DK to DK-AuNPs did not have a cytotoxic effect on HaCaT cells. Overproduction of ROS may result in cell death,

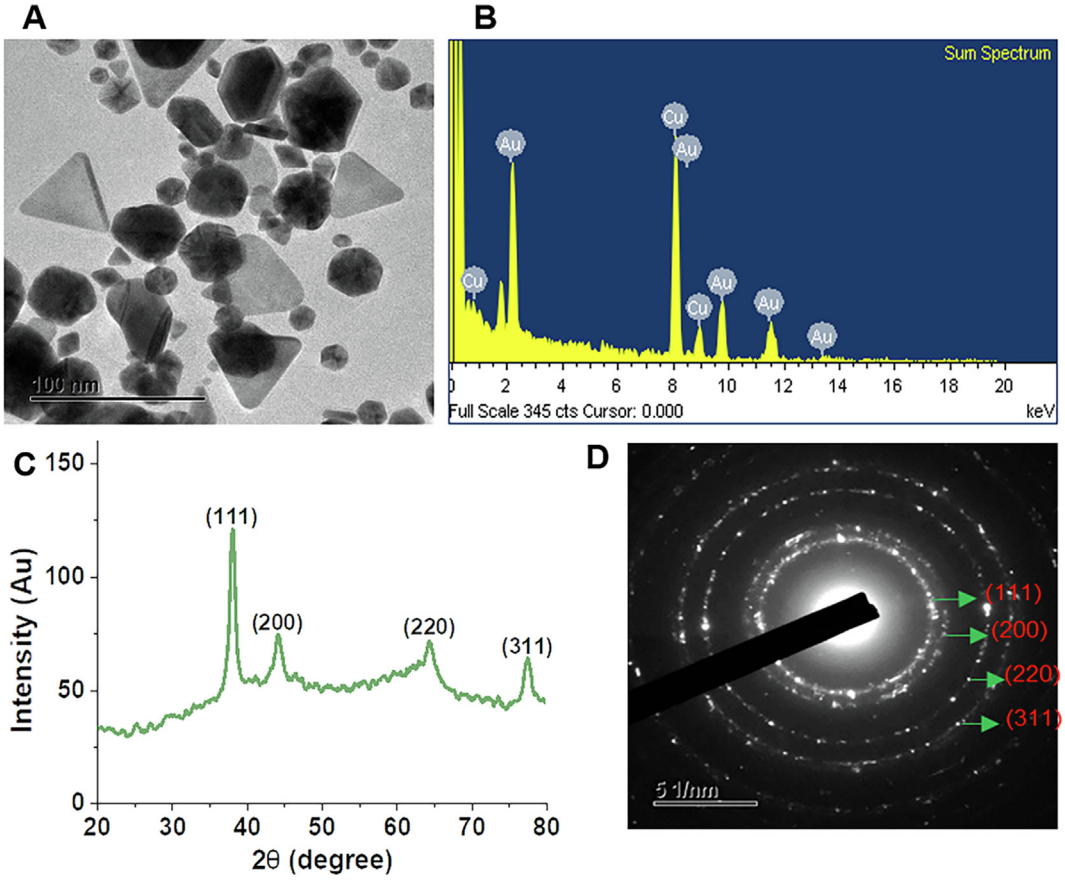

Fig. 2 DK-AuNPs physicochemical characterization. (A) Transmission electron microscopy (TEM) picture was used for determining the morphological properties of DK-AuNPs. (B) Energy-dispersive X-ray (EDX) spectrum. (C) X-ray diffraction (XRD) spectrum for crystalline structure determination. (D) A TEM image of selected area electron diffraction (SAED) was used for determining the crystalline structure of DK-AuNPs.

mitochondrial malfunction, and protein degradation (Di Meo et al., 2016). To determine functional changes in mitochondria, we measured ROS generation in cells and mitochondria. T + I treatment increased Mito-SOX and intracellular ROS secretion, whereas DK-AuNPs, DK, and PC (20 ng/mL) decreased Mito-SOX and ROS generation in a dose-dependently at 100 and 200 µg/mL (Fig. 5A-B). Our results showed that DK-AuNPs significantly decreased the generation of Mito-SOX and ROS in HaCaT cells compared to DK and PC.

3.3. Skin anti-inflammatory potential of DK-AuNPs

3.3.1. Inhibition of pro-inflammatory cytokines and chemokines

Chemokines have a major impact on the activation of inflammatory regulators, and T cells or leukocytes are employed to inflamed skin regions as a response. Moreover, cytokines and chemokines, such as interleukin 8 (IL-8), interleukin 6 (IL-6), CC chemokine ligand 17 (CCL17)/ thymus and activation-regulated chemokine (TARC), have been linked to the recruitment of Th2 type cells and high levels of chemokine expression in dermatitis (Yang et al., 2015). Thus, the secretion of proinflammatory cytokines and chemokines in HaCaT cells after exposure to T + I was assessed using ELISA. The release of cytokines and chemokines in the supernatant significantly increased following T + I (10 ng/mL) treatment for 24 h, whereas DK-AuNPs pretreatment (100 and 200 µg/mL) resulted in a decrease in T + I induced production compared to treatment with DK and PC (Fig. 6A-C). Therefore, ELISA results showed that DK-AuNPs and DK were effective in preventing T + I induced elevation of IL-8, IL-6, and TARC production.

3.3.2. Cytokines and chemokines mRNA gene expression

Human keratinocytes are associated with inflammation through the expression of the pro-inflammatory cytokines *IL-8* and *IL-6*, chemokines (*CCL17*/*TARC*, C—C motif chemokine ligand 27 *(CCL27)*/ cutaneous T cell-attracting chemokine *(CTACK)* and Chemokine (C—C motif) ligand 5 (*CCL5*)/ normal T cell expressed and presumably secreted (*RANTES)*), which is a large supergene of pro-inflammatory cytokines, and is expressed in activated T cells, platelets, airway epithelial cells, and fibroblasts. *RANTES*, *CTACK*, and *TARC* secretion have a major impact on the development of inflammatory conditions (Cho et al., 2020). Therefore, we used quantitative real-time PCR to examine HaCaT cells that had been pretreated with DK-AuNPs, DK, and PC for 1 h before exposure to T + I for 24 h and to determine whether the mRNA expression of proinflammatory cytokines and

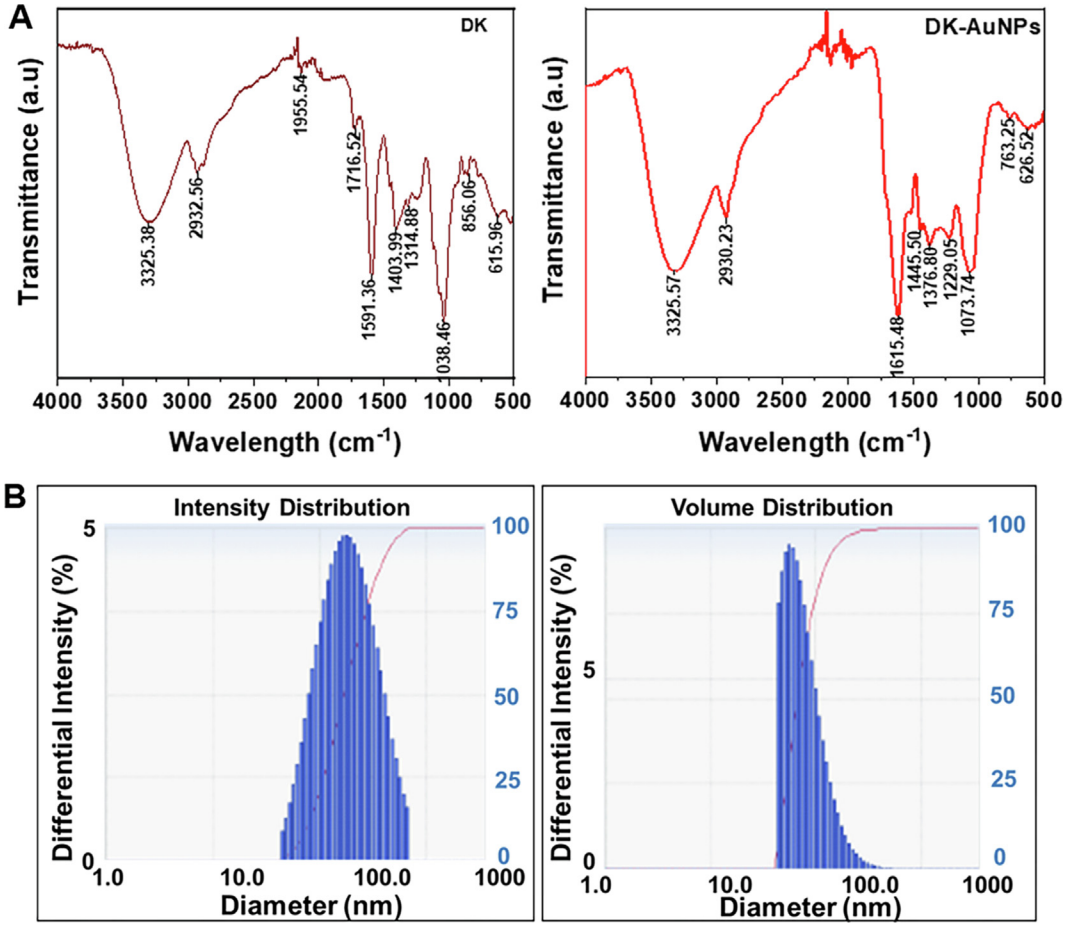

Fig. 3 (A) Infrared absorption spectrum produced by Fourier-transform infrared (FT-IR) spectrum for confirmation of chemical linkage confirmation in DK-AuNPs. (B) The intensity and volume distributions of DK-AuNPs were determined using dynamic light scattering (DLS) spectrum.

chemokines was suppressed. In comparison to DK and PC, DK-AuNPs downregulated the gene regulation of *IL-6*, *IL-8*, *TARC*/*CCL17*, *RANTES*/*CCL15*, and *CTACK*/*CCL27*, in T + I induced HaCaT cells, which was consistent with the ELISA result (Fig. 7A-E). Notably, DK-AuNPs (200 μg/mL) showed a better inhibitory effect than PC. Therefore, these results suggest that DK-AuNPs can recover T + I stimulated HaCaT cells and that it could reverse the inflammation in HaCaT cells.

3.3.3. MAPKs/NF-κB signalling pathways in HaCaT cells

Keratinocytes have a diverse set of cell surface receptors, including TNF-α and IFN-γ, two receptors that may crosslink when stimulated. In inflammatory skin diseases, T + I simultaneously enhances keratinocyte cytokine production (Jayasinghe et al., 2022). Several studies have indicated that T + I stimulates the synthesis of chemokines and cytokines including *RANTES, TARC, CTACK, IL-6*, and *IL-8,* in human epidermal keratinocytes. This may cause the development and activation of mitogen-activated protein kinase (MAPKs) and nuclear factor kappa light chain enhancer of activated B cells (NF-κB) signaling pathways in cells, which are linked to inflammatory responses (Mehta et al., 2017). MAPKs (p38 kinase (p38), extracellular signal-regulated kinase (ERK), and c-Jun *N*-terminal kinase (JNK)) affect the pathophysiology of inflammatory reactions (Lim et al., 2018). Generally, MAPKs control gene expression upstream of the NF-κB, which regulates genes and mediators associated with inflammation (Ge et al., 2021). All these variables actively contribute to the enhancement of pathogenesis in patients with dermatitis. Fig. 8A presents the effect of DK-AuNPs/DK (100 and 200 μg/mL) on the protein expression and activity of MAPKs such as p38, ERK, and JNK in T + I stimulated HaCaT cells. To determine whether DK-AuNPs and DK influenced MAPK phosphorylation, we measured the relative protein concentrations of p-ERK/ERK, p-p38/p-38, and p-JNK/JNK (Fig. 8B). DK-AuNPs exhibited no effect on total protein levels but showed a strong inhibitory effect on the phosphorylation of p38, ERK, and JNK in T + I induced HaCaT cells. As part of our investigation into the potential effects of DK-AuNPs/DK on the NF-κB signaling pathway, we measured the levels of nuclear factor of kappa light polypeptide gene

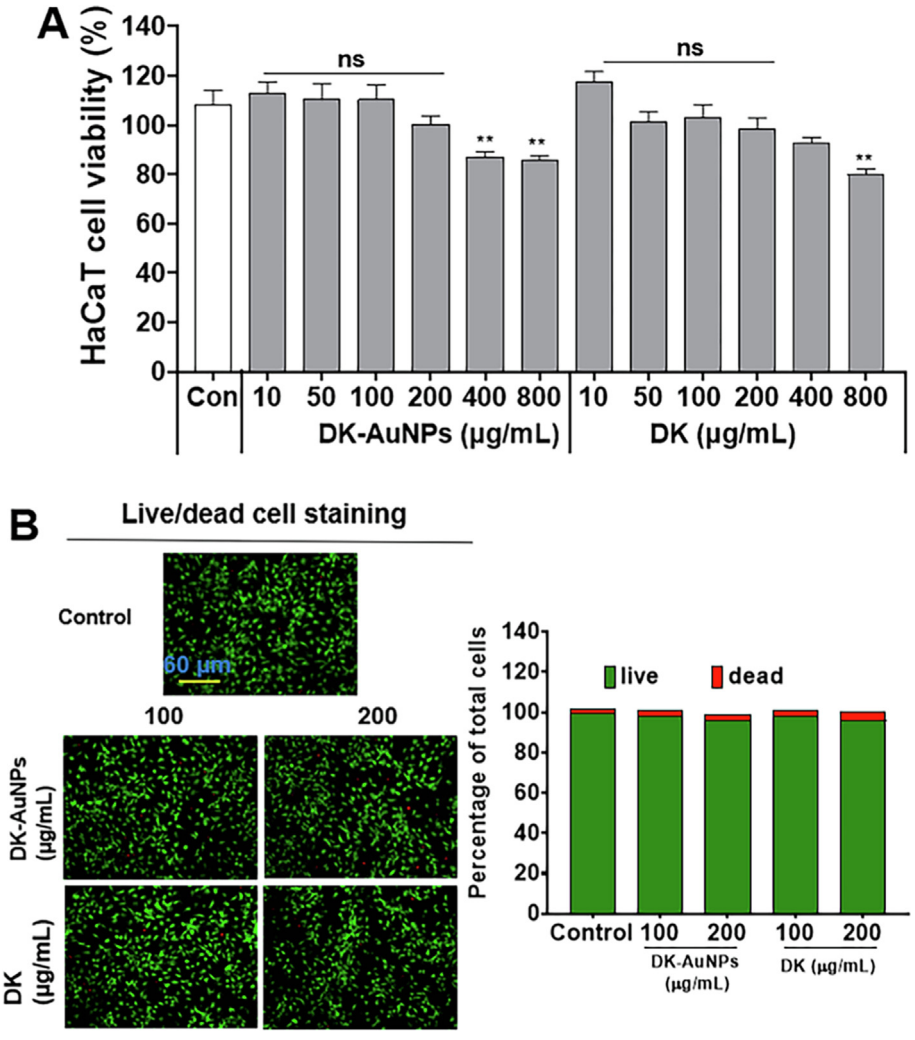

Fig. 4 Cytotoxic effect of DK-AuNPs and DK, against human epidermal keratinocytes. (A) Cytotoxicity of indicated concentrations of DK-AuNPs and DK on HaCaT cells, as determined using MTT assay; (B) LIVE and DEAD staining in DK-AuNPs and DK treated HaCaT cells.

enhancer in B-cells inhibitor, alpha (IκB-α) degradation and *P*65 phosphorylation. When T + I induced proinflammatory cytokines and chemokines are produced in HaCaT cells, NF-κB is involved in the transcriptional control of these molecules. DK-AuNPs restored IκB-α protein expression, which had been decreased by T + I (Fig. 9A-B). Moreover, inducible inflammatory cytokines, the release of which is induced by NF-κB, particularly Inducible nitric oxide synthase (iNOS) and Cyclooxygenase 2 (COX-2), are key mediators of the cutaneous inflammatory response (Liu et al., 2018). In contrast to DK, DK-AuNPs significantly reduced the activation of NF-κB by degradation of IκB-α, iNOS, and COX-2 without changing the total protein levels in the existence of T + I. These results indicated DK-AuNPs can promote the anti-inflammation activity through inhibition MAPKs/NF-κB signaling pathway.

3.4. Skin moisturizing activity by treating DK-AuNPs

3.4.1. Hyaluronic acid production

Normal skin function and health are both dependent on sufficient moisture, which is also a critical aspect of preserving skin health. HA is a large and dense polymer that is presented on the top layer of skin. Owing to its ability to retain water, HA is used in many special skin hydration treatments (Marinho et al., 2021). Mammalian cells have three distinct Hyaluronan synthase (HAS) isoforms (*HAS1, HAS2*, and *HAS3*), each of which has a distinct catalytic activity or is present in a distinct cell type (Gruber et al., 2022). Among these isoforms, *HAS1* exhibits the highest enzymatic activity followed by *HAS2* and *HAS3*. *HAS2* is the most strongly expressed isoform in keratinocytes and is significantly suppressed in the skin of elderly individuals. Activation of the Akt signaling pathway in fro/fro mouse fibroblasts has been reported to lead to an increase in *HAS2* mRNA expression, which was associated with elevated HA production. Compound K has been reported to enhance by stimulating the production of HA in HaCaT cells. By activating the ERK and Akt mechanisms, which in response increased HAS2 levels and facilitated the production of HA. Therefore, by regulating HA synthesis in the skin, modulation of *HAS2* expression in keratinocytes may aid in preserving skin hydration and homeostasis. Here, we determined whether DK-AuNPs could increase HA synthesis. According to ELISA results in Fig. 10A, DK-AuNPs significantly increased the synthesis of HA. Additionally, the qRT-PCR results (Fig. 10B-D), showed that DK-AuNPs significantly increased the gene expression levels of *HAS1, HAS2*, and *HAS3* compared with DK and PC (*N*-acetylglucosamine (NAE – 5 mg/mL)). Moreover, *HYAL*s are the primary enzymes responsible for the breakdown of HA *via* activation of specific processes. Many studies

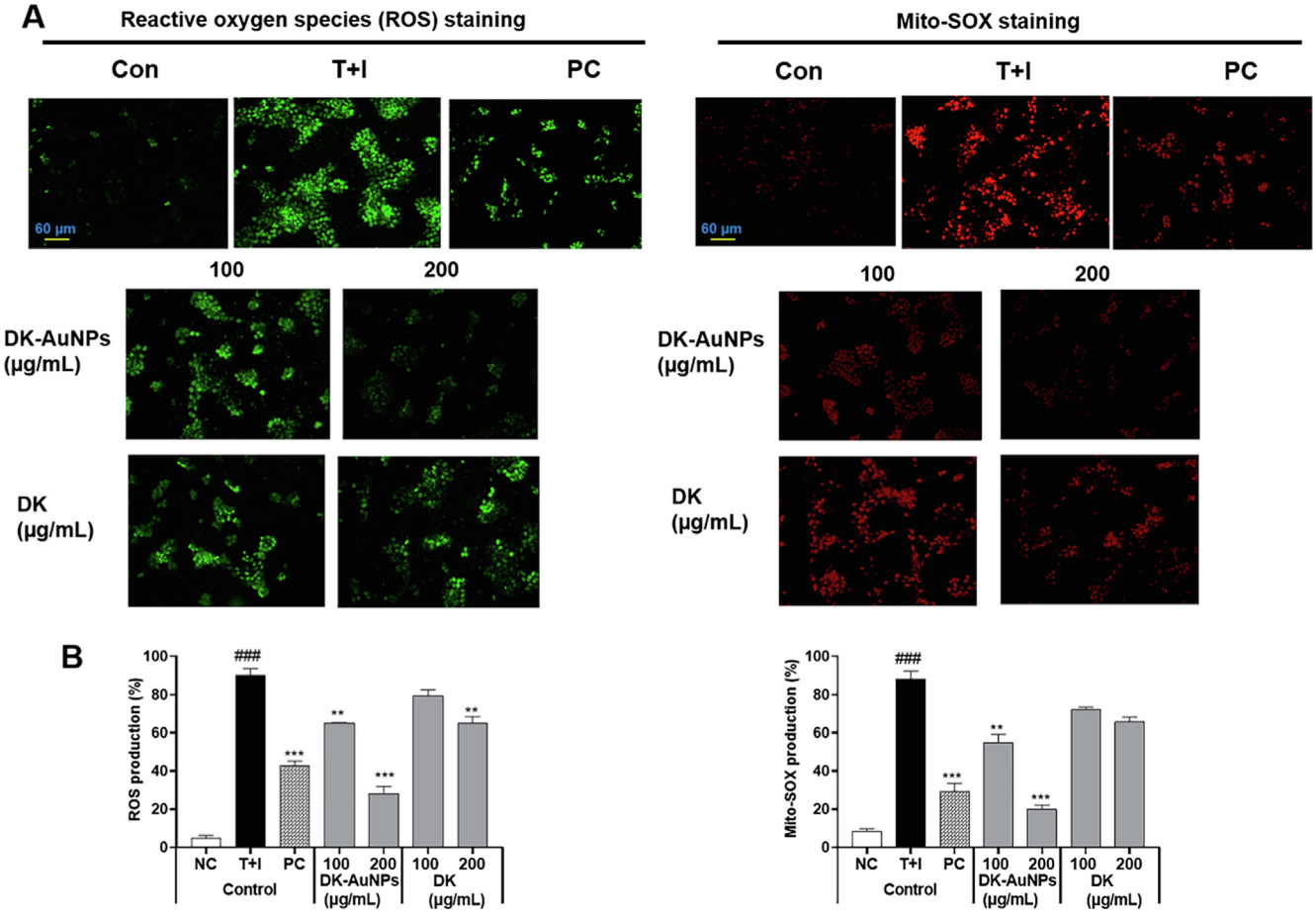

Fig. 5 (A) Fluorescence microscopic images of DK-AuNPs and DK treated HaCaT cells stained for reactive oxygen species (ROS) and Mito-SOX. (B) Results were quantified using the Image J software. Asterisks in the column indicate significant differences between sample and control *, #, $p < 0.05$; **, ##, $p < 0.01$; ***, ###, $p < 0.001$; ns, not significant.

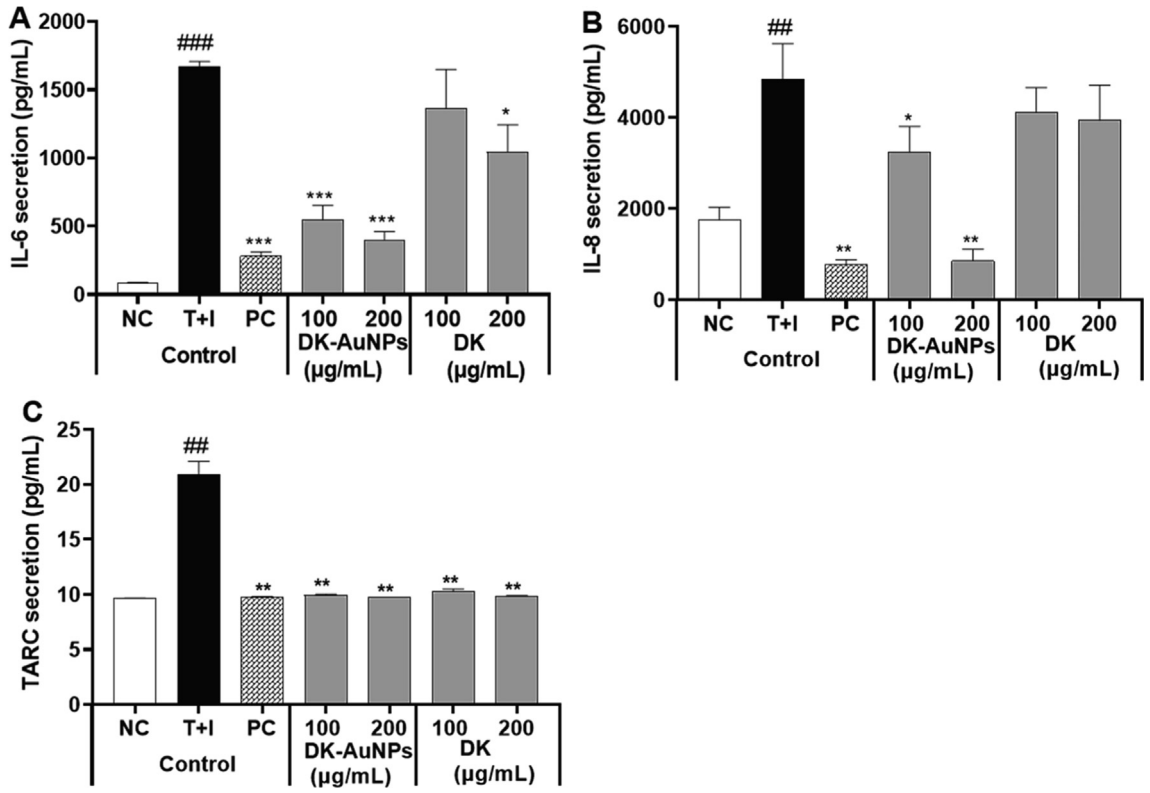

Fig. 6 Effect of DK-AuNPs on the production of pro-inflammatory cytokines in T + I stimulated HaCaT cells. The production of (A) IL-6, (B) IL-8, and (C) TARC was measured using ELISA. Asterisks in the column indicate significant differences between sample and control *, #, $p < 0.05$; **, ##, $p < 0.01$; ***, ###, $p < 0.001$; ns, not significant.

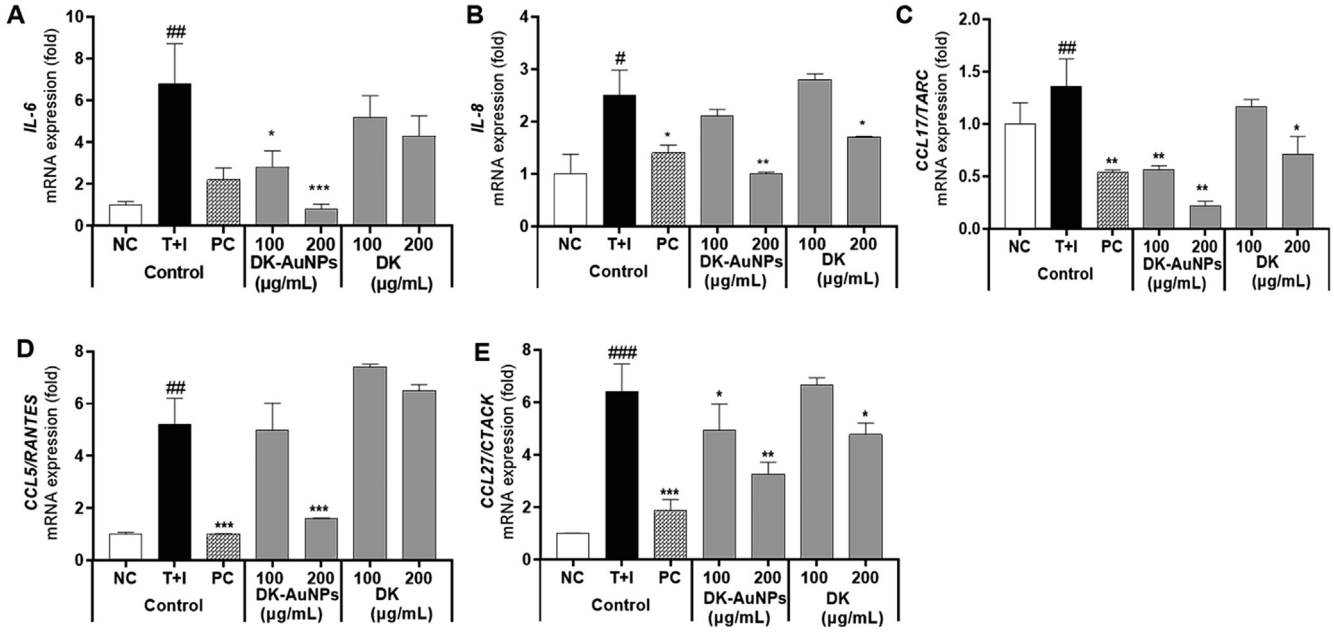

Fig. 7 Effect of DK-AuNPs on the relative gene expression of pro-inflammatory cytokines in T + I stimulated HaCaT cells. The relative mRNA expression of (A) *IL-6*, (B) *IL-8*, (C) *CCL-17*/*TARC*, (D) *CCL15*/*RANTES*, and (E) *CCL-27*/*CTACK* were measured using qRT-PCR analysis. Asterisks in the column indicate significant differences between sample and control *, #, $p < 0.05$; **, ##, $p < 0.01$; ***, ###, $p < 0.001$; ns, not significant.

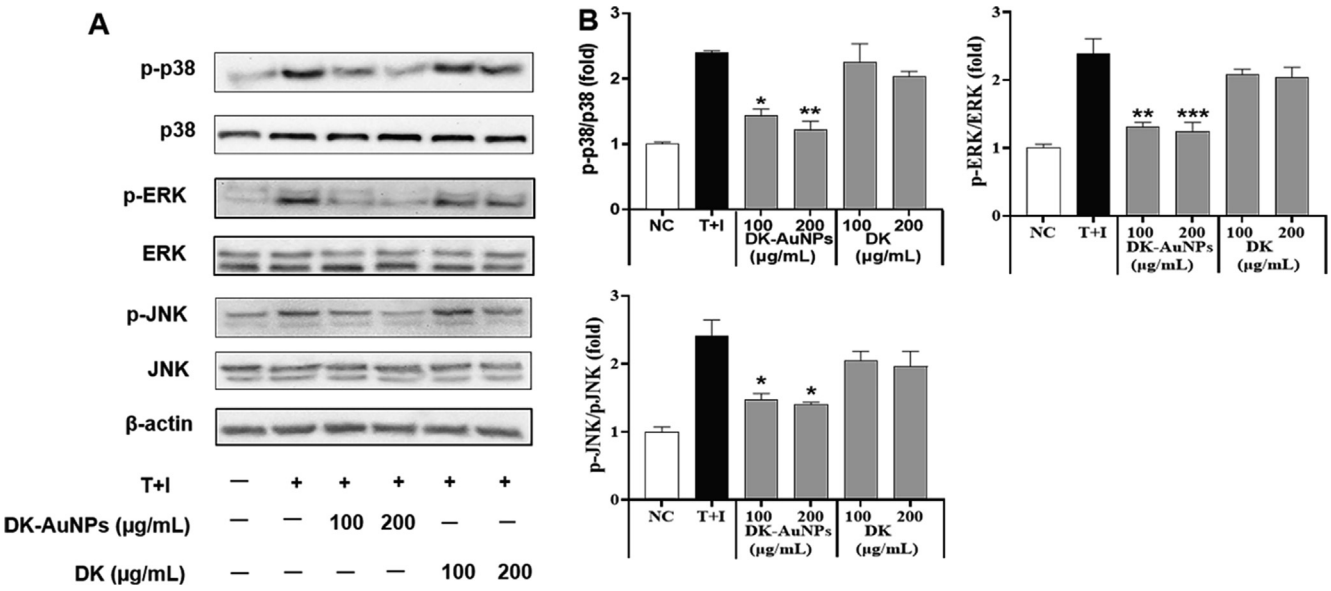

Fig. 8 Effect of DK-AuNPs on the expression of mitogen-activated protein kinase (MAPKs) in TNF-α/IFN-γ-stimulated HaCaT cells. (A) Protein expression of p38, ERK, and JNK phosphorylation in HaCaT cells was detected by western blotting. (B) Results were quantified using the Image J software. Asterisks in the column indicate significant differences between sample and control *, #, $p < 0.05$; **, ##, $p < 0.01$; ***, ###, $p < 0.001$; ns, not significant.

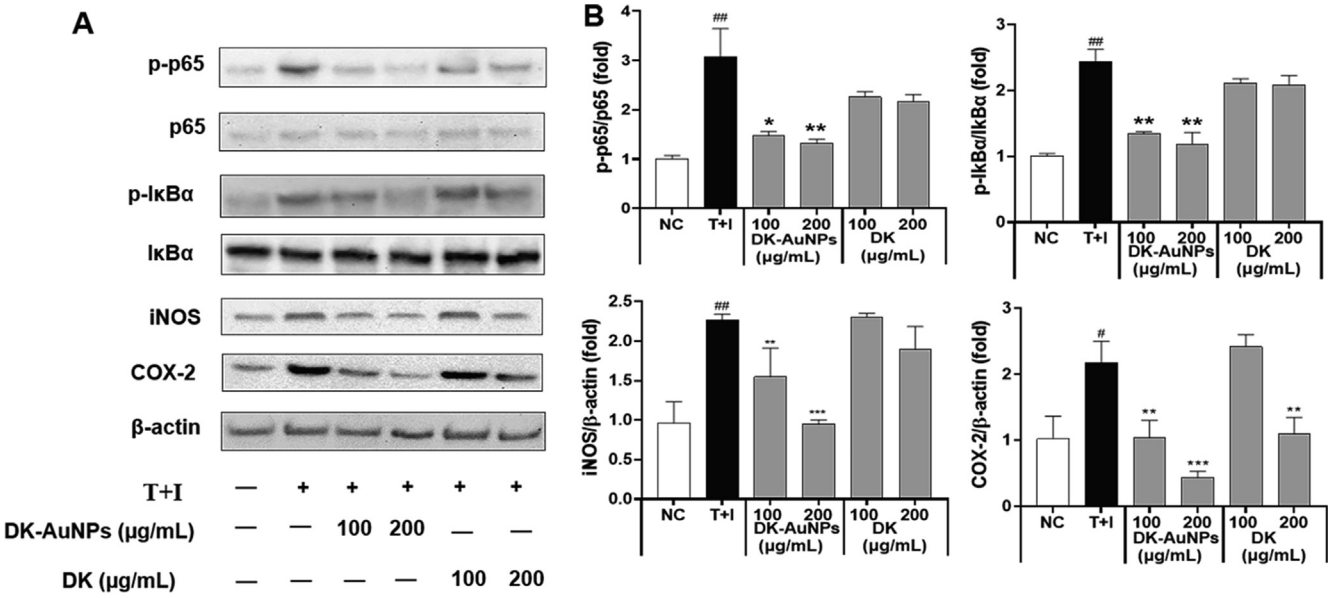

Fig. 9 Effect of DK-AuNPs on NF-κB translocation in T + I stimulated HaCaT cells. (A) Protein expression of p65, IκBα, iNOS, and COX-2 in HaCaT cells. (B) Results were quantified using the Image J software. Asterisks in the column indicate significant differences between sample and control *, #, $p < 0.05$; **, ##, $p < 0.01$; ***, ###, $p < 0.001$; ns, not significant.

have indicated that hyaluronidase 1 (*HYAL1*) breaks down HA polysaccharides into di- and tetra-saccharides (Caon et al., 2021). *HYAL1* is expressed in keratinocytes in the granular layer of the skin. In contrast, *HYAL2* is structurally similar to *HYAL1*; however, its activity and localization differ. The *HYAL2* enzyme is found in epidermis cell membranes. As shown in (Fig. 10E-F), the gene expression levels of *HYAL1* and *HYAL2* in the DK-AuNP treated HaCaT cells were significantly suppressed compared to that in DK and PC treated cells. Therefore, these results suggest that DK-AuNPs can suppress *HYAL1/2* expression and promote HAS regulation in HaCaT cells indicating that DK-AuNPs have potential skin moisturizing activity.

3.4.2. PI3K/Akt signaling pathway by HAS2 regulation

Furthermore, the phosphatidylinositol 3-kinase (PI3K)/ protein kinase B (Akt) signaling pathway is a key condition for the production of HAS2 in human skin cells (Mi et al., 2022). The activation of PI3K/Akt results in the sequential phosphorylation and activation of inhibitor kappa-B kinase

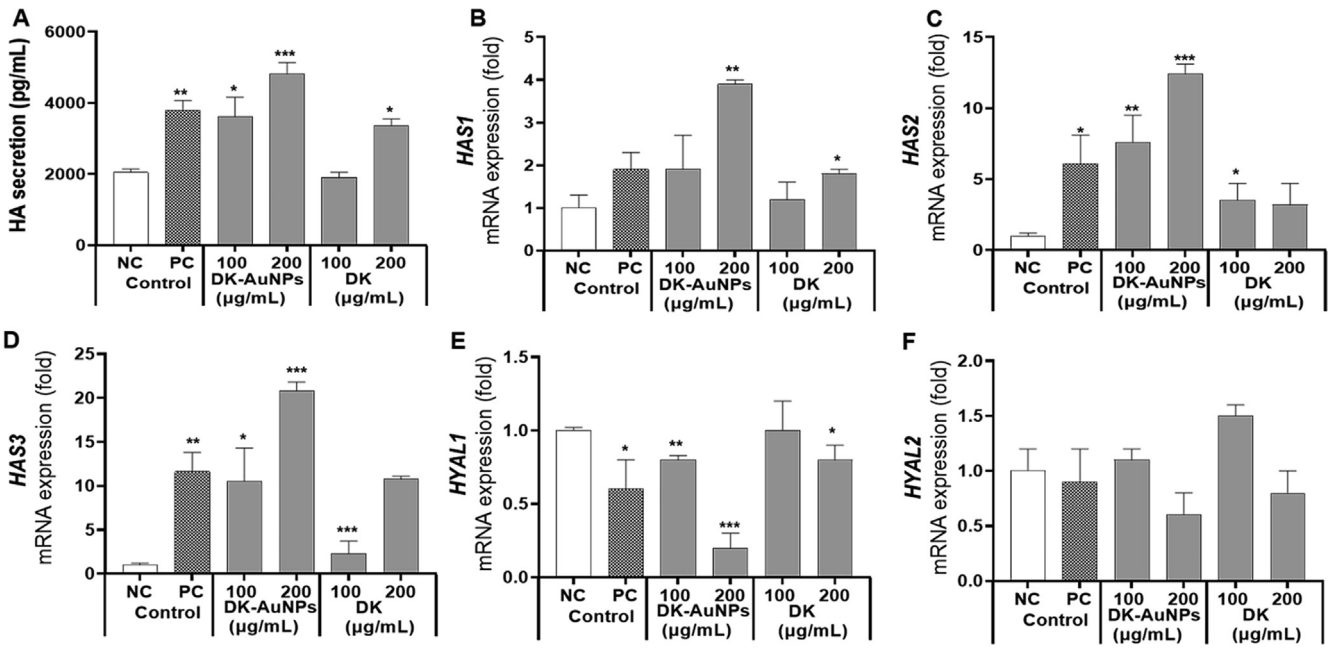

Fig. 10 Effect of DK-AuNPs on hyaluronic acid (HA) production in HaCaT cells. (A) The production of HA was measured using ELISA. The mRNA gene expression of (B) *HAS1*, (C) *HAS2,* (D) *HAS3*, (E) *HYAL1*, and (F) *HYAL2* were measured using qRT-PCR analysis. Asterisks in the column indicate significant differences between sample and control control *, #, $p < 0.05$; **, ##, $p < 0.01$; ***, ###, $p < 0.001$; ns, not significant.

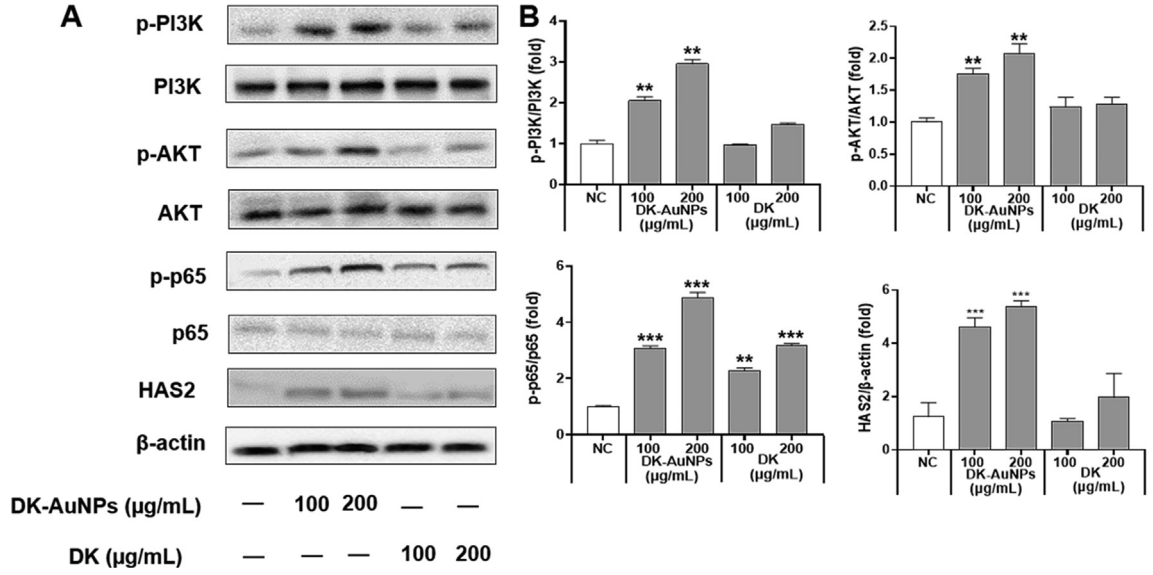

Fig. 11 Effect of DK-AuNPs on the PI3K/AKT signaling pathway in HaCaT cells. (A) Protein expression of PI3k, AKT, p65, and HAS2 in HaCaT cells. (B) Results were quantified using the Image J software. Asterisks in the column indicate significant differences between sample and control *, #, $p < 0.05$; **, ##, $p < 0.01$; ***, ###, $p < 0.001$; ns, not significant.

alpha/beta (IKK/beta) and inhibitor kappa B alpha (IκBα). When phosphorylated IκBα is degraded by ubiquitination, the resultant nuclear factor immunoglobulin kappa chain enhancer B (NF-κB) is released from the complex with IκBα and activated, and the production of the target protein is enhanced as a transcription factor (Lee et al., 2019). Thus, NF-κB is involved in the expression of human HAS2. We explored whether DK and DK-AuNP drove HAS2 involvement in PI3K/Akt signaling pathway that activates NF-κB (Fig. 11A). DK-AuNPs significantly upregulated PI3K and Akt phosphorylation along with p65 by promoting HAS2 expression in a dose-dependent manner. Fig. 11B presents the expression of related proteins determined using the Image J software. Therefore, our results indicate that DK-AuNPs can regulate PI3K/Akt/NF-κB activation by enhancing HAS2 expression. These findings, in combination with the anti-inflammatory activities of DK-AuNPs, support the potential therapeutic benefits of DK-AuNPs against reduced skin mois-

ture and degradation of the epidermal barrier function in T + I induced inflammation in HaCaT keratinocytes.

3.5. Determination of phytochemicals for the syntheizes of DK-AuNPs

The primary active phytochemicals in DK were identified using a UPLC-MS/MS study. Photodiode array (PDA) chromatogram and base peak chromatogram (BPC) of DK are shown in (Fig. S1A and B), respectively. By examining an in-house spectrum library, mass spectrometry (MS) and tandem MS (MS2) was utilized to determine the mass to charge ratio (m/z) and putatively identify the principal peaks with a mass accuracy < 5 ppm. Four peaks on the BPC at retention periods of 2.47, 3.57, 5.8, and 8.22 min were verified to match with their source ions at 221.0435, 247.0802, 294.1562, and 294.1562, respectively, according to MS analysis in positive ionized mode ([M + H] +). Several bioactive compounds were found in DK, but only the main natural compounds such as purpurogallin, ranunculin, were presented, along with other unknown compounds. According to spectral library, the substance found in the DK extract at RT (min)-8.22 was probably fenamic acid/salicylanilide. However, these substances are not natural, so this could be an unknown compound. Notabally, purpurogallin is the major compound identified in DK extract, which has been previously shown to have antioxidant, anticancer, and anti-inflammatory activities (Zhang et al., 2022). Therefore, these compounds might take part in synthesizing DK-AuNPs and also influence the activity of anti-inflammatory or HA synthesis.

4. Conclusion

This study develops AuNPs to aid in the healing process of skin diseases. Thus, DK fruit extracts primary phytochemicals converted DK-AuNPs in an ecologically friendly plant-mediated synthesis. Several characterization techniques was performed to confirm the physicalchemical properties of the synthesized DK-AuNPs. The DK-AuNPs showed nontoxic effect in HaCaT cells until 200 μg/mL and it could inhibit ROS and Mito-SOX release in T + I-induced HaCaT cells. Moreover, the DK-AuNPs notably supressed the generation of inflammatory regulators in T + I-induced HaCaT cells; these effects were related to downregulation of the MAPK and NF-κB signaling pathways. The skin's moisturizing activity is an important factor for skin for which we analyzed the hyaluronic acid (HA) secretion along with HAS (1–3) and HYAL (1–2) biomarkers. Moreover, we evaluated the underlying mechanism of these activities through protein expression of the MAPK/NFκB signaling pathway for anti-inflammatory and PI3K/AKT/NFκB signaling pathways for HA production. Compare to the well know and commercialy available drugs such as DEX and NAG, the synthesized DK-AuNPs could be an ecologically and cost friendly skin disease treating agent. In addition, our findings support basic data for novel nanoparticles and evaluating their activities, which may lead to the development of medicines based on DK-AuNPs. Further *in vivo* mechanism and clinical trials need to be performed for exploreing the influence of DK-AuNPs on human health, particularly with regard to their safety.

CRediT authorship contribution statement

Sanjeevram Dhandapani: Formal analysis, Data curation, Writing – original draft. **Rongbo Wang:** Methodology, Data curation, Formal analysis. **Ki cheol Hwang:** Resources. **Hoon Kim:** Methodology. **Yeon-Ju Kim:** Project administration, Supervision.

Declaration of Competing Interest

The authors declare that they have no known competing financial interests or personal relationships that could have appeared to influence the work reported in this paper.

Acknowledgement

This work was supported by KDBIO Corp. and also was carried out with the support of "Cooperative Research Program for Agriculture Science and Technology Development (PJ01703502)" Rural Development Administration, Republic of Korea.

Appendix A. Supplementary material

Supplementary data to this article can be found online at https://doi.org/10.1016/j.arabjc.2023.104551.

References

Ahati, P., Xu, T., Chen, L., Fang, H., 2022. Biosynthesis, characterization and evaluation of anti-bone carcinoma, cytotoxicity, and antioxidant properties of gold nanoparticles mediated by Citrus reticulata seed aqueous extract: introducing a novel chemotherapeutic drug. Inorg. Chem. Commun. 143,. https://doi.org/10.1016/j.inoche.2022.109791 109791.

Akhtar, S., Asiri, S., Khan, F.A., Gunday, S., Iqbal, A., Alrushaid, N., Labib, O., Deen, G., Henari, F., 2022. Formulation of gold nanoparticles with hibiscus and curcumin extracts induced anticancer activity. Arab. J. Chem. 15, (2). https://doi.org/10.1016/j.arabjc.2021.103594 103594.

Asahina, R., Maeda, S., 2017. A review of the roles of keratinocyte-derived cytokines and chemokines in the pathogenesis of atopic dermatitis in humans and dogs. Adv. Vet. Dermatol. 8, 15–25. https://doi.org/10.1002/9781119278368.ch2.1.

Botteon, C., Silva, L., Ccana-Ccapatinta, G., Silva, T., Ambrosio, S., Veneziani, R., Bastos, J., Marcato, P., 2021. Biosynthesis and characterization of gold nanoparticles using Brazilian red propolis and evaluation of its antimicrobial and anticancer activities. Sci. Rep. 11 (1), 1–16. https://doi.org/10.1038/s41598-021-81281-w.

Caon, I., Parnigoni, A., Viola, M., Karousou, E., Passi, A., Vigetti, D., 2021. Cell energy metabolism and hyaluronan synthesis. J. Histochem. Cytochem. 69 (1), 35–47. https://doi.org/10.1369/0022155420929772.

Chen, Y., Feng, X., 2022. Gold nanoparticles for skin drug delivery. Int. J. Pharm. 122122. https://doi.org/10.1016/j.ijpharm.2022.122122.

Cho, S.-H., Kim, H.-S., Lee, W., Han, E.J., Kim, S.-Y., Fernando, I. S., Ahn, G., Kim, K.-N., 2020. Eckol from Ecklonia cava ameliorates TNF-α/IFN-γ-induced inflammatory responses via regulating MAPKs and NF-κB signaling pathway in HaCaT cells. Int. Immunopharmacol. 82,. https://doi.org/10.1016/j.intimp.2019.106146 106146.

Cho, N.H., Kim, Y.B., Lee, Y.Y., Im, S.W., Kim, R.M., Kim, J.W., Namgung, S.D., Lee, H.-E., Kim, H., Han, J.H., 2022. Adenine oligomer directed synthesis of chiral gold nanoparticles. Nat. Commun. 13 (1), 1–10. https://doi.org/10.1038/s41467-022-31513-y.

Contini, C., Hindley, J.W., Macdonald, T.J., Barritt, J.D., Ces, O., Quirke, N., 2020. Size dependency of gold nanoparticles interacting with model membranes. Commun. Chem. 3 (1), 1–12. https://doi.org/10.1038/s42004-020-00377-y.

Damiani, G., Eggenhöffner, R., Pigatto, P.D.M., Bragazzi, N.L., 2019. Nanotechnology meets atopic dermatitis: current solutions, challenges and future prospects. insights and implications from a systematic review of the literature. Bioact. Mater. 4, 380–386. https://doi.org/10.1016/j.bioactmat.2019.11.003.

Dhandapani, S., Xu, X., Wang, R., Puja, A.M., Kim, H., Perumalsamy, H., Balusamy, S.R., Kim, Y.-J., 2021. Biosynthesis of gold nanoparticles using Nigella sativa and Curtobacterium proimmune K3 and evaluation of their anticancer activity. Mater. Sci. Eng. C. 127,. https://doi.org/10.1016/j.msec.2021.112214 112214.

Di Meo, S., Reed, T.T., Venditti, P., Victor, V.M., 2016. Role of ROS and RNS sources in physiological and pathological conditions. Oxid. Med. Cell. 2016. https://doi.org/10.1155/2016/1245049.

Direito, R., Rocha, J., Serra, A.-T., Fernandes, A., Freitas, M., Fernandes, E., Pinto, R., Bronze, R., Sepodes, B., Figueira, M.-E., 2020. Anti-inflammatory effects of persimmon (Diospyros kaki L.) in experimental rodent rheumatoid arthritis. J Diet Suppl. 17 (6), 663–683. https://doi.org/10.1080/19390211.2019.1645256.

Doan, V.-D., Pham, Q.-H., Huynh, B.-A., Nguyen, A.-T., Nguyen, T.-D., 2021. Kinetic analysis of nitrophenol reduction and colourimetric detection of hydrogen peroxide based on gold nanoparticles catalyst biosynthesised from Cynomorium songaricum. J. Environ. Chem. Eng. 9, (6). https://doi.org/10.1016/j.jece.2021.106590 106590.

Ferrara, L., 2021. Persimmon (Diospyros kaki L.): nutritional importance and potential pharmacological activities of this ancient fruit. J. Softw. Eng. 7, 01–04.

Ferreira, K. C. B., Valle, A. B. C. d. S., Paes, C. Q., Tavares, G. D., Pittella, F., 2021. Nanostructured Lipid Carriers for the Formulation of Topical Anti-Inflammatory Nanomedicines Based on Natural Substances. Pharmaceutics. 13(9), 1454. https://doi.org/10.3390/pharmaceutics13091454.

Ge, J., Guo, K., Zhang, C., Talukder, M., Lv, M.-W., Li, J.-Y., Li, J.-L., 2021. Comparison of nanoparticle-selenium, selenium-enriched yeast and sodium selenite on the alleviation of cadmium-induced inflammation via NF-kB/IκB pathway in heart. Sci. Total Environ. 773,. https://doi.org/10.1016/j.scitotenv.2021.145442 145442.

Gessner, I., Park, J.H., Lin, H.Y., Lee, H., Weissleder, R., 2022. Magnetic gold nanoparticles with idealized coating for enhanced point-of-care sensing. Adv. Healthc. Mater. 11 (2), 2102035. https://doi.org/10.1002/adhm.202102035.

Gruber, J.V., Holtz, R., Riemer, J., 2022. Hyaluronic acid (HA) stimulates the in vitro expression of CD44 proteins but not HAS1 proteins in normal human epidermal keratinocytes (NHEKs) and is HA molecular weight dependent. J. Cosmet. Dermatol. 21 (3), 1193–1198. https://doi.org/10.1111/jocd.14188.

Hwang, K.C., Shin, H.Y., Kim, W.J., Seo, M.S., Kim, H., 2021. Effects of a high-molecular-weight polysaccharides isolated from Korean persimmon on the antioxidant, anti-inflammatory, and antiwrinkle activity. Molecules 26 (6), 1600. https://doi.org/10.3390/molecules26061600.

Iranpour Anaraki, N., Liebi, M., Ong, Q., Blanchet, C., Maurya, A. K., Stellacci, F., Salentinig, S., Wick, P., Neels, A., 2022. In-situ investigations on gold nanoparticles stabilization mechanisms in biological environments containing HSA. Adv. Funct. Mater. 32 (9), 2110253. https://doi.org/10.1002/adfm.202110253.

Jayasinghe, A.M.K., Kirindage, K.G.I.S., Fernando, I.P.S., Han, E.J., Oh, G.-W., Jung, W.-K., Ahn, G., 2022. Fucoidan isolated from sargassum confusum suppresses inflammatory responses and oxidative stress in TNF-α/IFN-γ-stimulated HaCaT keratinocytes by activating Nrf2/HO-1 signaling pathway. Mar. Drugs. 20 (2), 117. https://doi.org/10.3390/md20020117.

Kashif, M., Akhtar, N., Mustafa, R., 2017. An overview of dermatological and cosmeceutical benefits of Diospyros kaki and its phytoconstituents. Rev. Bras. Farmacogn. 27, 650–662. https://doi.org/10.1016/j.bjp.2017.06.004.

Kim, T.H., Kim, W.J., Park, S.Y., Kim, H., Chung, D.K., 2021. In vitro anti-wrinkle and skin-moisturizing effects of evening primrose (Oenothera biennis) sprout and identification of its active components. Processes 9 (1), 145. https://doi.org/10.3390/pr9010145.

Klonowska, J., Gleń, J., Nowicki, R.J., Trzeciak, M., 2018. New cytokines in the pathogenesis of atopic dermatitis new therapeutic targets. Int. J. Mol. Sci. 19 (10), 3086. https://doi.org/10.3390/ijms19103086.

Ko, W.-C., Wang, S.-J., Hsiao, C.-Y., Hung, C.-T., Hsu, Y.-J., Chang, D.-C., Hung, C.-F., 2022. Pharmacological role of functionalized gold nanoparticles in disease applications. Molecules 27 (5), 1551. https://doi.org/10.3390/molecules27051551.

Lee, J.-E., Kim, Y.-A., Yu, S., Park, S.Y., Kim, K.H., Kang, N.J., 2019. 3, 6-Anhydro-L-galactose increases hyaluronic acid production via the EGFR and AMPKα signaling pathway in HaCaT keratinocytes. J. Dermatol. Sci. 96 (2), 90–98. https://doi.org/10.1016/j.jdermsci.2019.10.005.

Lim, J.-M., Lee, B., Min, J.-H., Kim, E.-Y., Kim, J.-H., Hong, S., Kim, J.-J., Sohn, Y., Jung, H.-S., 2018. Effect of peiminine on DNCB-induced atopic dermatitis by inhibiting inflammatory cytokine expression in vivo and in vitro. Int. Immunopharmacol. 56, 135–142. https://doi.org/10.1016/j.intimp.2018.01.025.

Liu, W., Huang, S., Li, Y., Li, Y., Li, D., Wu, P., Wang, Q., Zheng, X., Zhang, K., 2018. Glycyrrhizic acid from licorice down-regulates inflammatory responses via blocking MAPK and PI3K/Akt-dependent NF-κB signalling pathways in TPA-induced skin inflammation. MedChemComm. 9 (9), 1502–1510. https://doi.org/10.1039/C8MD00288F.

Maalej, H., Maalej, A., Bayach, A., Zykwinska, A., Colliec-Jouault, S., Sinquin, C., Marchand, L., Ktari, N., Bardaa, S., Salah, R.B., 2022. A novel pectic polysaccharide-based hydrogel derived from okra (Abelmoschus esculentus L. Moench) for chronic diabetic wound healing. Eur. Polym. J., 111763 https://doi.org/10.1016/j.eurpolymj.2022.111763.

Marcelino, M.Y., Borges, F.A., Scorzoni, L., de Lacorte Singulani, J., Garms, B.C., Niemeyer, J.C., Guerra, N.B., Brasil, G.S.A.P., Mussagy, C.U., de Oliveira Carvalho, F.A., 2021. Synthesis and characterization of gold nanoparticles and their toxicity in alternative methods to the use of mammals. J. Environ. Chem. Eng. 9, (6). https://doi.org/10.1016/j.jece.2021.106779 106779.

Marinho, A., Nunes, C., Reis, S., 2021. Hyaluronic acid: a key ingredient in the therapy of inflammation. Biomolecules 11 (10), 1518. https://doi.org/10.3390/biom11101518.

Matheus, J. R. V., Andrade, C. J. d., Miyahira, R. F., Fai, A. E. C., 2020. Persimmon (Diospyros Kaki L.): chemical properties, bioactive compounds and potential use in the development of new products–a review. Food Rev. 1-18. https://doi.org/10.1080/87559129.2020.1733597.

Mehta, N.N., Teague, H.L., Swindell, W.R., Baumer, Y., Ward, N.L., Xing, X., Baugous, B., Johnston, A., Joshi, A.A., Silverman, J., 2017. IFN-γ and TNF-α synergism may provide a link between psoriasis and inflammatory atherogenesis. Sci. Rep. 7 (1), 1–11. https://doi.org/10.1038/s41598-017-14365-1.

Mi, X.-J., Kim, J.-K., Lee, S., Moon, S.-K., Kim, Y.-J., Kim, H., 2022. In vitro assessment of the anti-inflammatory and skin-moisturizing effects of Filipendula palmata (Pall.) Maxim. On human keratinocytes and identification of its bioactive phytochemicals. J. Ethnopharmacol. 296, 115523. https://doi.org/10.1016/j.jep.2022.115523.

Mirzaei, H., Khataminfar, S., Mohammadparast, S., Sales, S.S., Maftouh, M., Mohammadi, M., Simonian, M., Parizadeh, S.M., Hassanian, S.M., Avan, A., 2016. Circulating microRNAs as potential diagnostic biomarkers and therapeutic targets in gastric cancer: current status and future perspectives. Curr. Med. Chem. 23 (36), 4135–4150. https://doi.org/10.2174/0929867323666160818093854.

Mishra, B., Kumar, A., Tripathi, B.P., 2020. Polydopamine mediated in situ synthesis of highly dispersed gold nanoparticles for continuous flow catalysis and environmental remediation. J. Environ. Chem. Eng. 8, (5). https://doi.org/10.1016/j.jece.2020.104397 104397.

Nagaraj, B., Musthafa, S.A., Muhammad, S., Munuswamy-Ramanujam, G., Chung, W.J., Alodaini, H.A., Hatamleh, A.A., Al-Dosary, M.A., Ranganathan, V., 2022. Anti-microbial and anti-cancer activity of gold nanoparticles phytofabricated using clerodin enriched clerodendrum ethanolic leaf extract. J. King Saud Univ. Sci. 34, (4). https://doi.org/10.1016/j.jksus.2022.101989 101989.

Pradeep, M., Kruszka, D., Kachlicki, P., Mondal, D., Franklin, G., 2021. Uncovering the phytochemical basis and the mechanism of plant extract-mediated eco-friendly synthesis of silver nanoparticles using ultra-performance liquid chromatography coupled with a photodiode array and high-resolution mass spectrometry. ACS Sustain. Chem. Eng. 10 (1), 562–571. https://doi.org/10.1021/acssuschemeng.1c06960.

Qu, J., Yang, J., Chen, M., Zhai, A., 2022. Anti-human gastric cancer study of gold nanoparticles synthesized using Alhagi maurorum. Inorg. Chem. Commun., 109859 https://doi.org/10.1016/j.inoche.2022.109859.

Rujido-Santos, I., Naveiro-Seijo, L., Herbello-Hermelo, P., del Carmen Barciela-Alonso, M., Bermejo-Barrera, P., Moreda-Piñeiro, A., 2019. Silver nanoparticles assessment in moisturizing creams by ultrasound assisted extraction followed by sp-ICP-MS. Talanta 197, 530–538. https://doi.org/10.1016/j.talanta.2019.01.068.

Sanjeevram, D., Xu, X., Wang, R., Puja, A.M., Kim, H., Perumalsamy, H., Balusamy, S.R., Kim, Y.-J., 2021. Biosynthesis of gold nanoparticles using Nigella sativa and Curtobacterium proimmune K3 and evaluation of their anticancer activity. Mater. Sci. Eng. C, 112214. https://doi.org/10.1016/j.msec.2021.112214.

Schwartz-Duval, A.S., Konopka, C.J., Moitra, P., Daza, E.A., Srivastava, I., Johnson, E.V., Kampert, T.L., Fayn, S., Haran, A., Dobrucki, L.W., 2020. Intratumoral generation of photothermal gold nanoparticles through a vectorized biomineralization of ionic gold. Nat. Commun. 11 (1), 1–18. https://doi.org/10.1038/s41467-020-17595-6.

Sekar, V., Al-Ansari, M.M., Narenkumar, J., Al-Humaid, L., Arunkumar, P., Santhanam, A., 2022. Synthesis of gold nanoparticles (AuNPs) with improved anti-diabetic, antioxidant and anti-microbial activity from Physalis minima. J. King Saud Univ. Sci. 34, (6). https://doi.org/10.1016/j.jksus.2022.102197 102197.

Shin, H.Y., Hwang, K.C., Mi, X.J., Moon, S.K., Kim, Y.J., Kim, H., 2022. Rhamnogalacturonan I-rich polysaccharide isolated from fermented persimmon fruit increases macrophage-stimulatory activity by activating MAPK and NF-κB signaling. J. Sci. Food Agric. 102 (7), 2846–2854. https://doi.org/10.1002/jsfa.11625.

Song, W.C., Kim, B., Park, S.Y., Park, G., Oh, J.-W., 2022. Biosynthesis of silver and gold nanoparticles using Sargassum horneri extract as catalyst for industrial dye degradation. Arab. J. Chem. 15, (9). https://doi.org/10.1016/j.arabjc.2022.104056 104056.

Torres, T., Ferreira, E., Gonçalo, M., Mendes-Bastos, P., Selores, M., Filipe, P., 2019. Update on atopic dermatitis. Acta Med. Port. 32 (9), 606–613. https://doi.org/10.20344/amp.11963.

Vandarkuzhali, S.A.A., Karthikeyan, G., Pachamuthu, M., 2021. Microwave assisted biosynthesis of Borassus flabellifer fruit mediated silver and gold nanoparticles for dye reduction, antibacterial and anticancer activity. J. Environ. Chem. Eng. 9, (6). https://doi.org/10.1016/j.jece.2021.106411 106411.

Wang, R., Xu, X., Puja, A. M., Perumalsamy, H., Balusamy, S. R., Kim, H., Kim, Y.-J., 2021. Gold Nanoparticles Prepared with Phyllanthus emblica Fruit Extract and Bifidobacterium animalis subsp. lactis Can Induce Apoptosis via Mitochondrial Impairment with Inhibition of Autophagy in the Human Gastric Carcinoma Cell Line AGS. Nanomaterials. 11(5), 1260. https://doi.org/10.3390/nano11051260.

Wang, M., Meng, Y., Zhu, H., Hu, Y., Chang-Peng, X., Chao, X., Li, W., Pan, C., Li, C., 2021. Green synthesized gold nanoparticles using Viola betonicifolia leaves extract: characterization, antimicrobial, antioxidant, and cytobiocompatible activities. Int. Nanomed. J. 16, 7319. https://doi.org/10.2147/ijn.s323524.

Wang, R., Moon, S.-K., Kim, W.-J., Dhandapani, S., Kim, H., Kim, Y.-J., 2022. Biologically synthesized rosa rugosa-based gold nanoparticles suppress skin inflammatory responses via MAPK and NF-κB signaling pathway in TNF-α/IFN-γ-induced HaCaT keratinocytes. ACS Omega 7 (40), 35951–35960. https://doi.org/10.1021/acsomega.2c04832.

Xu, X.Y., Tran, T.H.M., Perumalsamy, H., Sanjeevram, D., Kim, Y.-J., 2021. Biosynthetic gold nanoparticles of Hibiscus syriacus L. callus potentiates anti-inflammation efficacy via an autophagy-dependent mechanism. Mater. Sci. Eng. C 124,. https://doi.org/10.1016/j.msec.2021.112035 112035.

Xu, X.Y., Moon, S.-K., Kim, J.-K., Kim, W.J., Kim, Y.-J., Kim, H., 2022. Structural properties and anti-dermatitis effects of flavonoids-loaded gold nanoparticles prepared by Eupatorium japonicum. Front. Pharmacol. 13. https://doi.org/10.3389/fphar.2022.1055378.

Yang, J.-H., Hwang, Y.-H., Gu, M.-J., Cho, W.-K., Ma, J.Y., 2015. Ethanol extracts of Sanguisorba officinalis L. suppress TNF-α/IFN-γ-induced pro-inflammatory chemokine production in HaCaT cells. Phytomedicine 22 (14), 1262–1268. https://doi.org/10.1016/j.phymed.2015.09.006.

Zayadi, R.A., Bakar, F.A., 2020. Comparative study on stability, antioxidant and catalytic activities of bio-stabilized colloidal gold nanoparticles using microalgae and cyanobacteria. J. Environ. Chem. Eng. 8, (4). https://doi.org/10.1016/j.jece.2020.103843 103843.

Zhang, S., Wu, X., Xiao, Y., 2022. Conversion of lignin-derived 3-methoxycatechol to the natural product purpurogallin using bacterial P450 GcoAB and laccase CueO. Appl. Microbiol. Biotechnol. 106 (2), 593–603. https://doi.org/10.1007/s00253-021-11738-5.